



Contents lists available at ScienceDirect

## Quaternary International

journal homepage: [www.elsevier.com/locate/quaint](http://www.elsevier.com/locate/quaint)

## Premonsoon precipitation variability in Kumaon Himalaya, India over a perspective of ~300 years

Ram R. Yadav <sup>a,\*</sup>, Krishna G. Misra <sup>a</sup>, Bahadur S. Kotlia <sup>b</sup>, Neha Upreti <sup>b</sup>

<sup>a</sup> Birbal Sahni Institute of Palaeobotany, 53 University Road, Lucknow 226007, India

<sup>b</sup> Department of Geology, Kumaon University, Nainital 263002, India

### ARTICLE INFO

#### Article history:

Available online xxx

### ABSTRACT

Variability in premonsoon precipitation, which has direct impact on rabi crop productivity in the Himalayan region, is not well understood in a long-term perspective, largely due to the paucity of weather data. We developed an annually resolved February–May (FM) precipitation record extending back to AD 1730 using tree-ring width data of Himalayan cedar for the first time from the Kumaon region, eastern sector of the western Himalaya, India. The FM precipitation reconstruction, capturing 58% of the variance in instrumental data over the calibration period (1901–1968), is the strongest so far from the Indian region. The reconstruction revealed inter-annual to decadal-scale variations in precipitation anomalies. Twentieth-century decadal-scale droughts occurred in the 1920s, and 1960s to early 1970s, and pluvials in the 1910s and 1980s. However, the droughts in 1920–1924 were the most severe of any other comparable period in last three centuries. Pre-instrumental droughts of the 1740s, 1780s, and 1840s were widespread in a large part of the western Himalaya. The drying tendency noted in the last two decades, which is widespread in the western Himalaya and western Nepal, in view of increased hydrological demand is alarming, and could cause severe water stress in the region unless adaptive measures are taken.

© 2013 Elsevier Ltd and INQUA. All rights reserved.

### 1. Introduction

The economy of the hill states in India is prone to the vagaries of climate, as infrastructure facilities in orography dominated regions are poorly developed. The agriculture system in Kumaon (28°44′–30°49′N; 78°45′–81°05′E), eastern region of western Himalaya, is highly vulnerable to precipitation variation, as only ~10% of the cultivated land is under irrigation (Sati, 2005) and rest is rain-fed. In view of this, understanding the natural pattern of precipitation and its predictability is much needed to evolve sustainable agricultural plans. However, this is seriously hampered due to limited weather data available from the region, which at the most extends back to beginning of the 20th century, and for only a few stations. High variability in precipitation in the orographically-dominated Himalayan region further limits the utility of spatially restricted weather data in understanding regional variability in precipitation.

High-resolution tree-ring records are available from the arid to semi-arid regions of the western Himalaya (Borgaonkar et al., 1994; Yadav and Park, 2000; Singh and Yadav, 2005; Singh et al., 2006, 2009; Yadav, 2011a,b, 2013; Yadav and Bhutiyani, 2013). Such studies from the eastern part of the western Himalaya, which is relatively wetter, are not available, largely due to the lack of old conifer trees in contrast to those found in north-western regions of the Himalaya. The weak climatic signal noted in ring-width chronologies of *Abies pindrow* and *Picea smithiana* growing in moist temperate forests in Kumaon has also been responsible for the slow pace of dendroclimatic studies in this region (Yadav, unpublished data).

The present work was initiated with the objective to develop long-term precipitation records for the Kumaon region using tree-ring data of Himalayan cedar, planted several centuries ago around temple complexes. The ring-width chronologies of Himalayan cedar (*Cedrus deodara*) from two sites in Kumaon were analysed for the first time to explore their dendroclimatic potential. Veracity and strength of the reconstruction was established by comparing it with instrumental weather data and proxy climate records available from adjacent regions. Such long-term climate records should be of profound socioeconomic

\* Corresponding author.

E-mail address: [rryadav2000@gmail.com](mailto:rryadav2000@gmail.com) (R.R. Yadav).

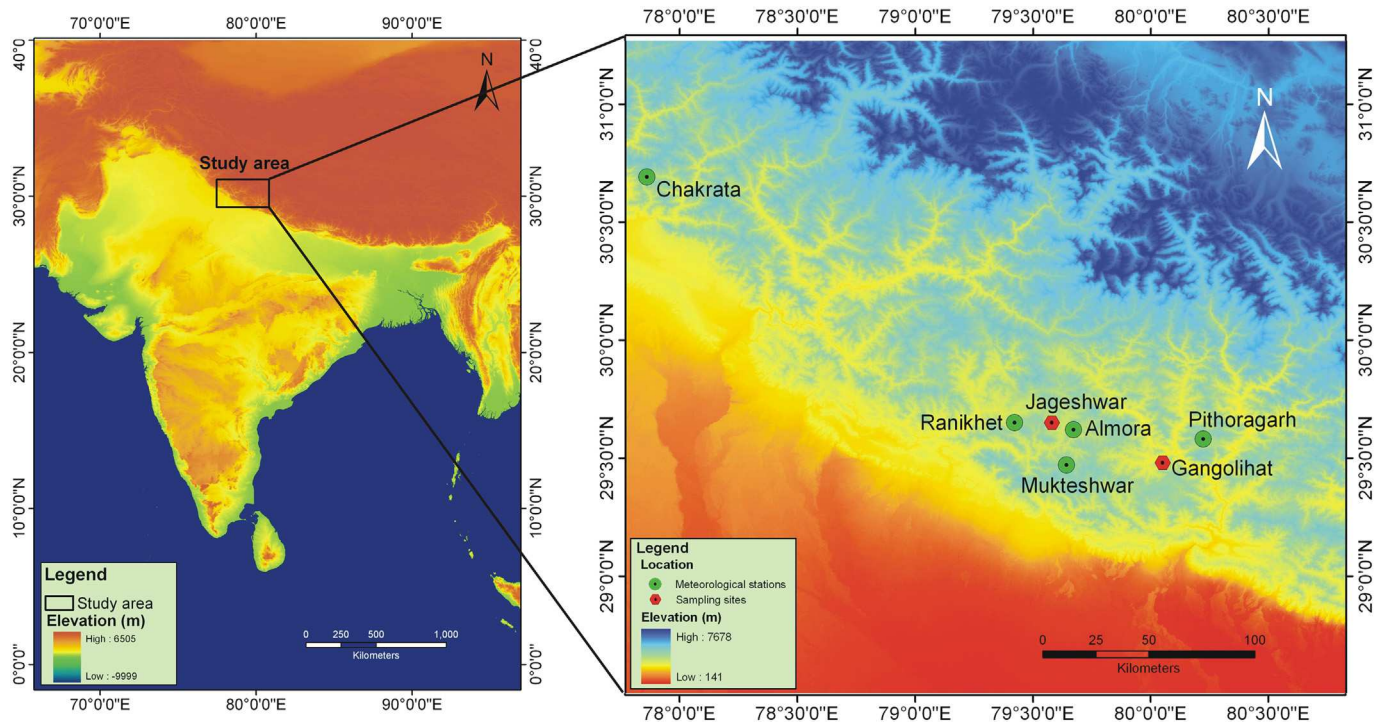


Fig. 1. Map showing the locations of the tree-ring sampling sites of the Himalayan cedar and meteorological stations used in present study.

significance, as these provide valuable insight to evolve sustainable agriculture and hydrological resource management plans for the region.

## 2. Data and methods

### 2.1. Tree-ring data

Vegetation in Kumaon region of the western Himalaya, depending on varying topography from outer Siwalik to the inner high Himalayas, ranges from sub-tropical to alpine (Champion and Seth, 1968). Many of the trees growing in these forests, especially conifers, are known to have datable growth rings. Himalayan cedar trees, very old in semi-arid to arid regions of the western Himalaya (Singh et al., 2004), are restricted to some disjunct locations in Kumaon, and are believed to have spread from plantations near the temples (Champion and Seth, 1968). In Hindu mythology, the Himalayan cedar is known for its grand appearance, and is treated as sacred and most preferred tree to be planted in temple complexes. The Jageshwar temple, a Hindu pilgrimage dedicated to Lord Shiva, built ~9th–13th centuries AD, is believed to be the first home of Himalayan cedar outside its natural habitat in the Himalayan region.

The Himalayan cedar forest stands in Jageshwar and Gangolihat in Kumaon were surveyed, and increment core samples from old trees collected for the first time in May 2013 (Fig. 1). Attempts were made to collect cores from undisturbed trees at breast height (~1.4 m) from directions at 90° to the slope. Usually, two cores were collected from healthy, undisturbed trees from both sites. The increment core samples were processed and growth ring sequences dated using the skeleton plot method (Stokes and Smiley, 1968; Fritts, 1976). Very good coherence in growth pattern of trees from two sites as revealed in COFECHA (Holmes, 1983) (mean  $r = 0.62–0.63$ ) and year-to-year similarity in ring-width plots indicates that

large-scale common regional climate signals affected growth of the trees over two sites.

The tree-ring chronologies of Himalayan cedar were developed using established dendrochronological procedures (Fritts, 1976). To select an appropriate detrending method, ring-width measurement plots of trees from different sites were carefully studied. The ring-width plots of tree samples from both the sites revealed that the Himalayan cedar growth over the sampling sites is influenced by stand dynamic features such as changing competition due to gap formations. Therefore, to maximize the common signal among the samples, we detrended the ring-width measurement series by using 50-year cubic spline with a 50% frequency response function cut off (Cook and Peters, 1981). However, prior to detrending, the ring-width measurement series were power transformed to stabilize variance in the heteroscedastic tree-ring-width measurement series (Cook and Peters, 1997). The growth trends were removed from the power transformed individual measurement series by subtraction, which minimizes the end fitting-type bias as compared to the ratios. In order to reduce the influence of outliers, the detrended ring-width measurement series of respective tree series were averaged to a mean chronology (standard) by computing the biweight robust mean (Cook, 1985). Another set of chronology was prepared where low-order autocorrelation from detrended series was removed using autoregressive moving average (ARMA) modelling, and the resulting residual series averaged to a mean site chronology by computing the biweight robust mean (Cook, 1985). The replication of 12 and 15 tree samples in chronologies from Jageshwar and Gangolihat respectively were found to be sufficient to achieve expressed population signal (eps) (Wigley et al., 1984) level of 0.85. The statistics of standard versions of two site chronologies are given in Table 1. Significant correlation among site chronologies for the common period 1730–2012 with eps level >0.85 ( $r = 0.75$ ,  $p < 0.0001$ ) suggests common environmental forcing affecting growth dynamics of trees over the respective sites.

**Table 1**

Chronology (standard) statistics of Himalayan cedar from two sites in Kumaon. The details of site locations are shown in Fig. 1. SY – start year of the chronology, EPS – expressed population signal, MI – mean index, MS – mean sensitivity, SD – standard deviation, AR1 – first order autocorrelation.

S. No.	Site	Location	Elevation (m)	Cores/trees	SY	Chronology with EPS >0.85	MI	MS	SD	AR1
1	Gangolihat	29°39'N–80°01'E	1760	38/27	1668	1720–2012	0.986	0.210	0.192	0.145
2	Jageshwar	29°38'N–79°51'E	1851	41/37	1536	1690–2012	0.977	0.257	0.236	0.244

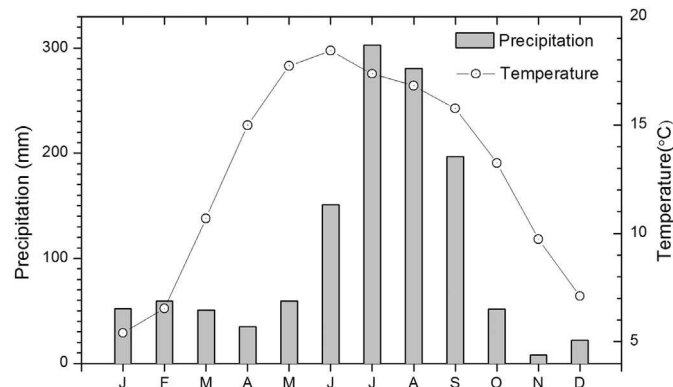


**Fig. 2.** Monthly precipitation and mean monthly temperature variations over Kumaon Himalaya, Uttarakhand.

## 2.2. Climate data

Weather records from Kumaon, analogous to other regions of the Himalaya, are spatially and temporally restricted. The longest weather record (temperature and precipitation) of Mukteshwar (29°28'N–79°38'E, 2171 m asl) in Nainital, Uttarakhand, close to the tree-ring sites extends back to AD 1897. The weather data of Mukteshwar show that bulk of precipitation (~73% of 1270 mm annual) occurs in monsoon season, spread over June–September (Fig. 2). The November–May precipitation, occurring largely due to western disturbances, is ~22% of the annual precipitation. Due to high spatial variability in precipitation in mountainous regions, single station data, which do not represent the regional climate features, are not suitable for calibration of tree-ring chronologies. In view of this, we prepared a regional mean precipitation series by merging data of five weather stations (Table 2). Averaging of multiple station series helps in minimizing the effect of errors and inhomogeneities at individual stations and maximization of regional and larger-scale climate features. The merging of data was guided by the existence of strong coherency in the precipitation data of five stations as measured by significant correlations (Table 3) and strong year-to-year similarity (Fig. 3). The monthly precipitation data of the five stations were merged to prepare the regional mean monthly series after normalization with reference to 1901–1968 common periods. The regional mean monthly precipitation series consisted of data from AD 1901–1968. The 1969–2011 precipitation data came from Mukteshwar station only. However, for temperature, the data were available only from Mukteshwar (AD 1897–1991). The temperature data of Mukteshwar show that June is the hottest month, with mean temperature ~18.4 °C, and January the coldest with mean temperature ~5.4 °C (Fig. 2).

**Table 2**

Meteorological stations used in preparing the mean regional precipitation series

Station	Latitude (N)	Longitude (E)	Altitude (m)	Length of record	Average FM precipitation (mm)
Almora	29°37'	79°40'	1651	1901–1968	163.4
Chakrata	30°41'	77°52'	2118	1901–1968	257.3
Mukteshwar	29°28'	79°38'	2171	1897–2011	199.0
Pithoragarh	29°35'	80°13'	1514	1901–1968	196.3
Ranikhet	29°39'	79°25'	1869	1901–1968	185.6

**Table 3**

Pearson correlation in FM precipitation of different stations. In every case two tailed *p* value is >0.0001.

	Almora	Chakrata	Mukteshwar	Pithoragarh
Chakrata	0.71			
Mukteshwar	0.88	0.72		
Pithoragarh	0.68	0.50	0.73	
Ranikhet	0.88	0.80	0.92	0.72

## 2.3. Climate signal in tree-ring data

To understand the climate signal contained in tree-ring data, the residual version of two site chronologies were used in response function analyses (Fritts, 1976). The monthly precipitation and temperature data from September of the previous year to September of the current year were used in correlation analyses with the two site residual chronologies. The correlations were calculated in two sub-periods (AD 1901–1968, 1969–1991) to understand temporal stability in the relationship. We noted similar relationships between tree-ring chronologies and climate variables in the two sub-periods, in spite of the temporally variable number of precipitation data sets used in developing the mean monthly regional series. The correlations between site chronologies and climate variables for AD 1901–1968 are depicted in Fig. 4, as larger replications of precipitation data sets (five series) were available for this period. The precipitation from previous year September to current year May showed direct relationship with the respective site chronologies. The correlations were consistently positive and significant ( $p < 0.05$ ) from February–May. However, no significant correlation was noted with precipitation during the monsoon months (June–September) when precipitation is prevalent in the region due to the active southwest summer monsoon. For temperature, the residual version of two site chronologies showed a negative relationship with the mean monthly temperature of Mukteshwar for most months, except summer monsoon months from July–September when it was positive. The correlation analyses revealed that a cool-moist condition in the premonsoon season is very important for the radial growth of Himalayan cedar trees in Kumaon. In view of the existence of significant correlation between ring-width chronologies and premonsoon precipitation, we used the regional mean February–May (FM) precipitation anomaly series for calibration with tree-ring data.

## 2.4. Calibration and reconstruction of February–May (FM) precipitation

Existence of a significantly positive and consistent relationship between residual version of two site chronologies of Himalayan cedar and regional mean FM precipitation series was taken as a guide to develop reconstruction. The residual chronologies of Himalayan cedar from both sites showed strong year-to-year variations with a distinct lack of long-term variations. Hence, to capture low frequency variations in the reconstruction, we used the standard version of two site chronologies in calibrations with the mean regional FM precipitation anomalies of five stations for 1901–1968.

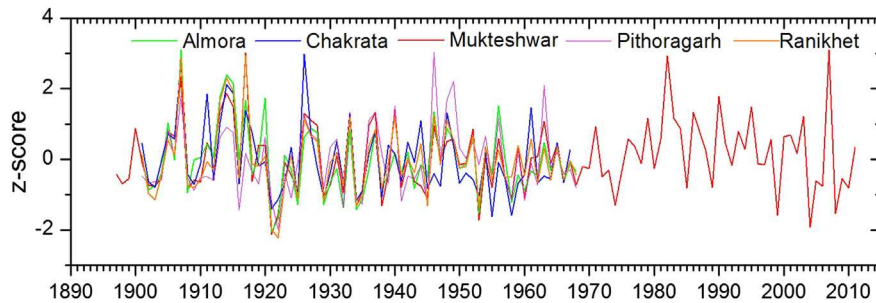


Fig. 3. FM precipitation of five stations plotted after normalization with respect to 1901–1968.

However, the precipitation series from AD 1969–2011, consisting of Mukteshwar data alone, were used for verification of the calibration model. In addition to  $t_0$  ring-width chronology variables, the lagged ( $t - 1$  and  $t + 1$ ) chronology variables were also tested to determine relationships with FM precipitation. The lagged chronology variables did not show a significant relationship with FM precipitation. Hence, only  $t_0$  chronology variables of the two series were used in calibration and reconstruction of FM precipitation. For this, we adopted principal component regression analysis for the common chronology period 1730–2012, for which sufficient sample replications were available in two site chronologies. The first principal component (PC#1), with eigenvalue 1.752 explaining 87.6% of the variance in the common chronology period AD 1730–2012, was used in calibrations with mean regional FM precipitation series. The two sub-period (1901–1968, 1969–2011) calibration and verification statistics, such as the reduction of error (RE), coefficient of efficiency (CE), Sign test, and Pearson correlation coefficient (Fritts, 1976; Cook et al., 1999) were used to test the significance and reliability of the reconstruction (Table 4, Fig. 5). Positive values of both the RE and the CE in verification periods denote statistical skill in the reconstruction. On establishment of the veracity of the calibration/verification statistics, we used the 1901–1968 calibration model for reconstruction, which captured 58% of the variance in the mean regional FM precipitation data. The reconstructed series revealed close year-to-year similarity and significant correlation with the mean regional FM precipitation series ( $r = 0.73$ , 1901–2011,  $p < 0.0001$ ).

younger than those in Jageshwar, indicating that the plantation of Himalayan cedar trees could have started first in the Jageshwar temple area, and gradually spread to other regions in Kumaon. The ring-width chronology statistics such as mean sensitivity (Table 1) and significant correlation between two site chronologies are analogous to other climate responsive Himalayan cedar chronologies developed in the western Himalayan region (Singh et al., 2004).

### 3.2. Analyses of FM precipitation reconstruction

The FM precipitation reconstruction extending back to AD 1730 superimposed with smoothed version of the reconstruction using 10 year low pass filter (Fig. 6) revealed strong year-to-year and decadal-scale variability. The reconstruction, capturing 58% of the variance in the regional mean precipitation series (1901–1968), is the strongest so far developed from the Himalayan region in India. Though most of the low precipitation events are well captured in the calibration model, the high precipitation events of 1906, 1917, 1982, and 2008 are relatively underestimated. In view of this, we emphasize the analyses of multiyear extremes, their causes and consequences in the following discussion. Nonetheless, high pre-monsoon precipitation events recorded in our data for 1877 and 1878, corroborated with high winter precipitation recorded in the Kumaon region (Atkinson, 1882), indicate considerable strength of the reconstruction in capturing extreme events. The reconstruction further revealed that extreme low precipitation events widely recorded in arid to cold-arid regions of the western Himalaya (Yadav

**Table 4**  
Calibration, verification statistics of February–May precipitation reconstruction;  $ar^2-r^2$  adjusted after degrees of freedom,  $R$  – Pearson correlation, Sign test, RE (reduction of error) and CE (coefficient of efficiency) (Fritts, 1976; Cook et al., 1999). The  $p$  values are given in parentheses.

S. No.	Period	Number of series	Calibration		Verification				
			Period	$ar^2$ (%)	Period	$R$	Sign test	RE	CE
1	1730–2012	2	1901–1968	58	1969–2011	0.694 (0.0001)	35 <sup>+</sup> /8 <sup>-</sup> (0.0000419)	0.391	0.364
			1969–2011	48	1901–1968	0.765 (0.0001)	52 <sup>+</sup> /16 <sup>-</sup> (0.0000141)	0.332	0.297
			1901–2011	53					

## 3. Results and discussion

### 3.1. Tree-ring-width chronology

Dating of Himalayan cedar tree core samples collected from two sites in Kumaon, outside its natural habitat, extends to AD 1536. In the Jageshwar forests, several snag woods were also recorded, the girth of which occasionally exceeded that of the sampled trees (~9 m). This indicates that the period of plantation of Himalayan cedar trees around the temple complexes could be even earlier than the early 16th century. The trees sampled from Gangolihat are relatively

and Park, 2000; Singh and Yadav, 2005; Singh et al., 2006; Yadav, 2011a,b) are also well represented in the relatively moist eastern part of the western Himalaya. The yearly distribution of extreme precipitation events ( $\pm 1$  standard deviation) revealed that most of the low precipitation events are found in the 1780s, 1890s, early 1920s, and late 1960s to early 1970s (Fig. 7). However, the pluvial events are concentrated in the 1730s, 1760s, 1820s, 1860s, 1910s, and 1980s. Interestingly these extreme premonsoon precipitation events were also recorded earlier in tree-ring-based precipitation reconstructions from the western Himalaya (Yadav, 2011a,b, 2013) indicating widespread occurrence across the Himalaya.

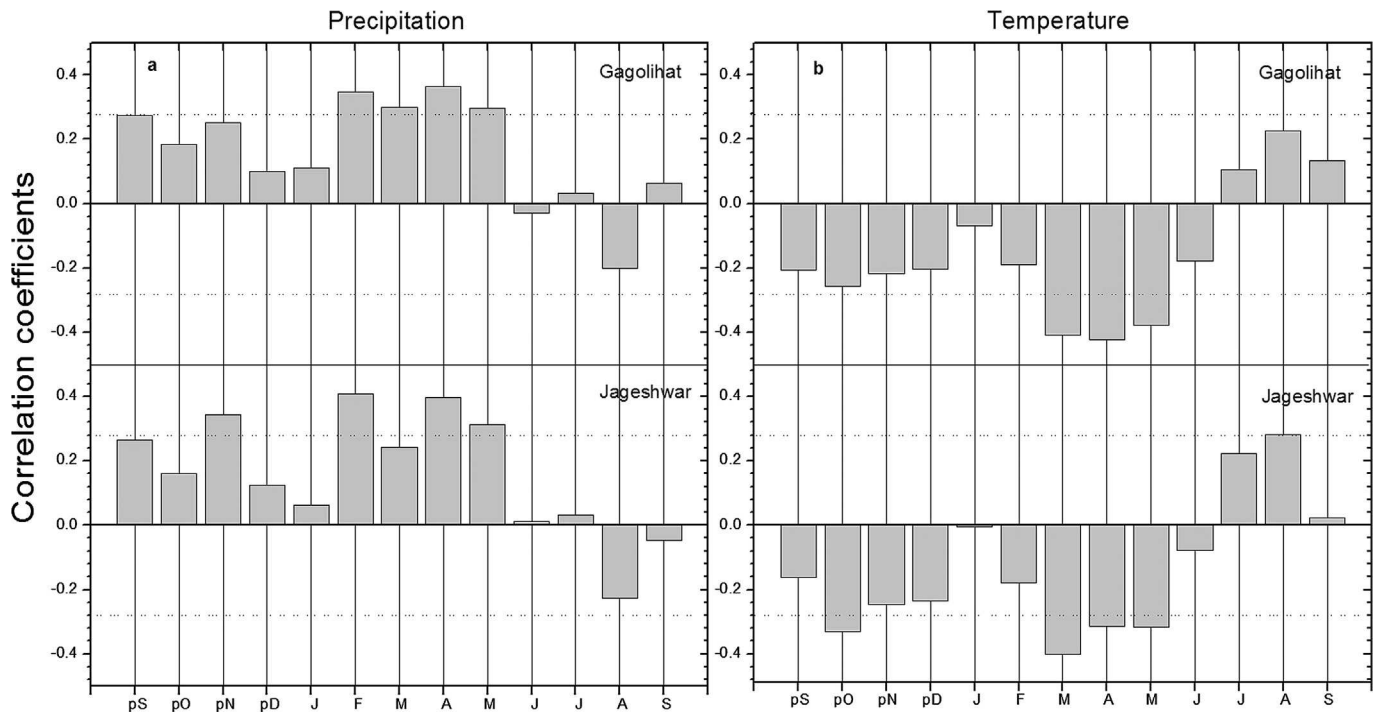


Fig. 4. Correlation functions of residual ring width chronology with mean regional precipitation series derived after merging five station data sets (a) and monthly Mukteshwar temperature (b) (bars above dotted lines are significant at 95% confidence level).

To understand distribution of longer episodes of sustained droughts and pluvial periods, the FM precipitation series was smoothed with 5 and 11-year running mean windows (Table 5). The most revealing pluvial phases in the 20th century occurred around 1910–1918, 1978–1988, and dry phases around 1920–1924, 1964–1974, and 1993–2001, which are consistent with the precipitation records from the region. Extreme dry and pluvial phases observed in our data are also reflected in March–May precipitation responsive tree-ring series of *Betula utilis* developed from Nepal Himalaya (Dawadi et al., 2013). The FM precipitation reconstruction as well as the observational records showed a distinct drying tendency since the 1990s (Fig. 6), when temperatures are also known to have increased (Dubey et al., 2003). The weather records from western Nepal have also indicated a downward trend in winter precipitation since 1995 (Wang et al., 2013). Such a drying tendency coupled with ongoing warming could seriously affect the availability of hydrological resources and thereby the socioeconomics of the region, where agriculture is predominantly rain-fed.

Table 5  
Dry and wet extremes of 5 and 11-years non-overlapping periods.

Dry		Wet	
Period	Anomaly	Period	Anomaly
<b>5-year mean</b>			
1920–1924	–2.53	1911–1915	3.68
1782–1786	–2.51	1788–1792	2.72
1744–1748	–2.30	1758–1762	2.32
1812–1816	–2.17	1979–1983	2.12
1972–1976	–2.07	1733–1737	1.76
1964–1968	–1.99	1751–1755	1.20
1846–1850	–1.57	1772–1776	1.18
1995–1999	–1.50	1862–1866	1.02
<b>11-year mean</b>			
1740–1750	–2.15	1909–1919	1.75
1964–1974	–1.72	1754–1764	1.34
1777–1787	–1.42	1978–1988	1.31
1916–1926	–0.85	1788–1798	1.06
1811–1821	–0.81	1822–1832	0.92

Pre-20th century pluvial phases were recorded in the 1730s, late 1750s to early 1760s, 1806–1810, 1823–1834, and 1860s, and dry phases in 1740s, 1780s, 1810s, late 1840s, and 1890s. To understand regional signatures in the present FM precipitation reconstruction, we compared our data with other reconstructions available from relatively drier regions of the western Himalaya (Yadav and Park, 2000; Singh and Yadav, 2005; Singh et al., 2006). A comparison of present FM precipitation reconstruction and tree-ring-based March–May precipitation reconstruction developed from Garhwal Himalaya (Singh et al., 2006) after 10-year low pass filtering revealed a close similarity on a decadal scale (Fig. 8). Nonetheless, there were distinct dissimilarities in two reconstructions towards the close of the 20th century. We are of the opinion that the increased March–May precipitation in late 20th century (Singh et al., 2006) could be possibly the artefact of methods used in detrending ring-width measurement series. The most significant droughts of the 1780s noted in our reconstruction have been found to be widespread in the western Himalayan region when low winter snowfall (Yadav and Bhutiyan, 2013), increased winter droughts (Yadav, 2013) and low Indus flow levels were recorded (Cook et al., 2013). Spatial correlation fields generated

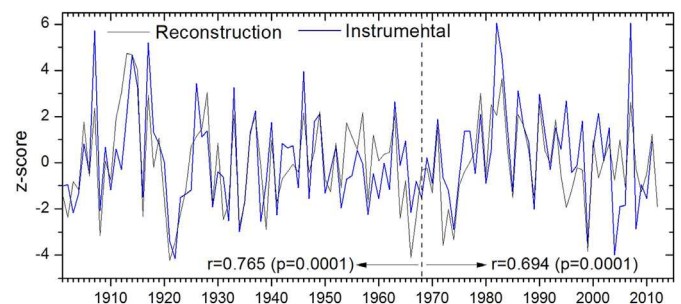
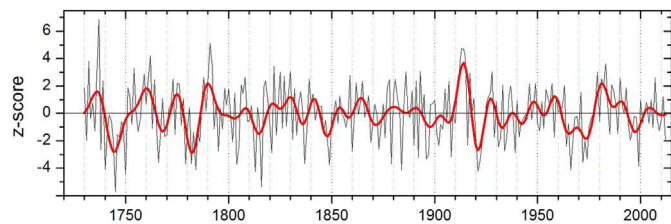
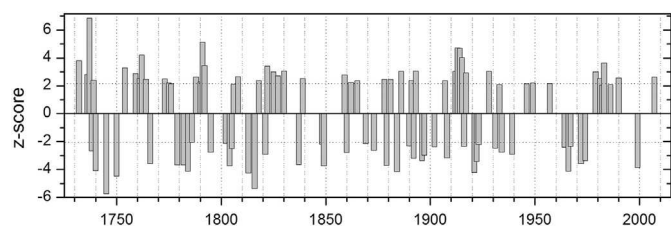


Fig. 5. Instrumental and reconstructed FM precipitation series plotted together for comparison (AD 1901–1968 calibration period was used in reconstruction).



**Fig. 6.** FM precipitation reconstruction (AD 1730–2012) for Kumaon Himalaya overlaid with 10-year low pass filtered version (thick line).



**Fig. 7.** Extreme precipitation values  $\pm$  one standard deviation.

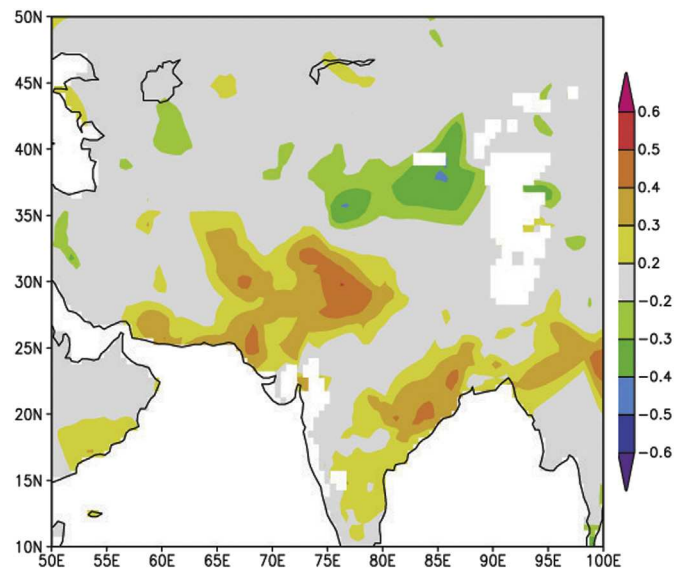


**Fig. 9.** Spatial correlation between reconstructed FM precipitation and gridded precipitation data (1969–2009). The picture was generated using the KNMI Climate Explorer program (<http://climexp.knmi.nl>; Oldenborgh and Burgers, 2005).

and early 20th centuries, whereas the  $\sim 32$ – $38$  years cycle is centred around the 1770s–1810s and 1930s–1960s.

#### 4. Conclusions

The present study developed ring-width chronologies of Himalayan cedar growing at two sites in Kumaon, eastern part of the western Himalaya, which fall outside its natural homeland. The chronologies from Jageshwar and Gangolihat in Kumaon extend to AD 1536 and 1668 respectively. These chronologies add to the existing chronology network from arid regions of the north-western Himalaya to the relatively moist eastern region of the western Himalaya. These tree-ring data could be integrated with the emerging tree-ring data network from the central Himalayan region of Nepal (Cook et al., 2003; Bräuning, 2004; Dawadi et al., 2013) to understand large-scale climate features.

The ring-width chronologies showing a significant positive relationship with FM precipitation were used to develop precipitation reconstruction extending back to AD 1730. The calibration model, capturing 58% of the variance in the observed regional precipitation series (1901–1968), is the strongest so far from the Himalayas in India, and helped in assessment of dry and pluvial phases over time and space. The most significant 20th century droughts occurred in 1920–1924, and the 1960s to early 1970s. The

using gridded precipitation data (CRU TS3 climate data available on <http://climexp.knmi.nl>; Oldenborgh and Burgers, 2005) and reconstructed FM precipitation (1969–2009) revealed large-scale precipitation signatures in our reconstruction (Fig. 9). Given the presence of regional scale patterns in our reconstruction, we used Multi Taper Spectral analysis (Mann and Lees, 1996) to examine the FM precipitation in the frequency domain (Fig. 10a). The analysis revealed a significant quasi-biennial oscillatory mode of  $\sim 2.2$ – $2.8$ , and periodicities of  $\sim 16$ , and 32–38 years. The longer term cycles in the FM precipitation reconstruction are not revealed, as tree-ring data were standardized using 50-year cubic spline with a 50% frequency response function cut off. The quasi-biennial oscillatory modes recorded in our data show characteristic periodicity of the tropical climate system, whereas  $\sim 16$  year cycles are close to the frequency domain of the Pacific Decadal Oscillation. The periodicity of  $\sim 32$ – $38$  years could be associated with the Atlantic Multi-decadal Oscillation (AMO) (Gray et al., 2004; Knight et al., 2005) as well as solar variability (Bruckner cycle; Raspopov et al., 2004). Interestingly, such multidecadal oscillations have also been reported earlier in observational winter precipitation records from northwestern India (Yadava et al., 2012) and spring precipitation reconstruction from the western Himalaya (Yadav, 2011a). To examine the stationarity of low-frequency modes, wavelet analysis (Torrence and Compo, 1998) on the full length of FM precipitation reconstruction was performed (Fig. 10b and c). The strong frequency components of  $\sim 16$  years cycle are centred on the late 18th

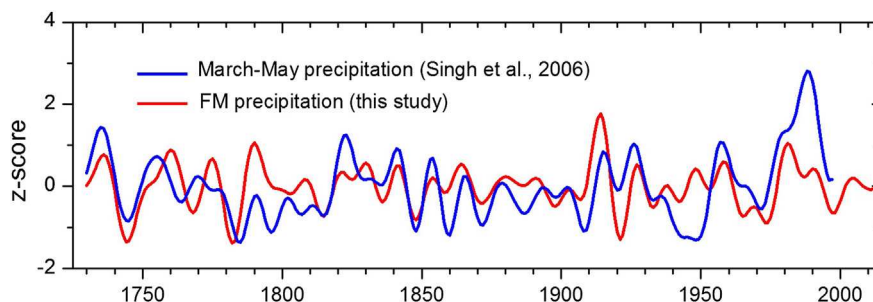


**Fig. 8.** FM precipitation reconstruction (present) from Kumaon region and March–May precipitation reconstruction from Garhwal region of the western Himalaya (Singh et al., 2006). The reconstructions were smoothed with 10-year low pass filter.

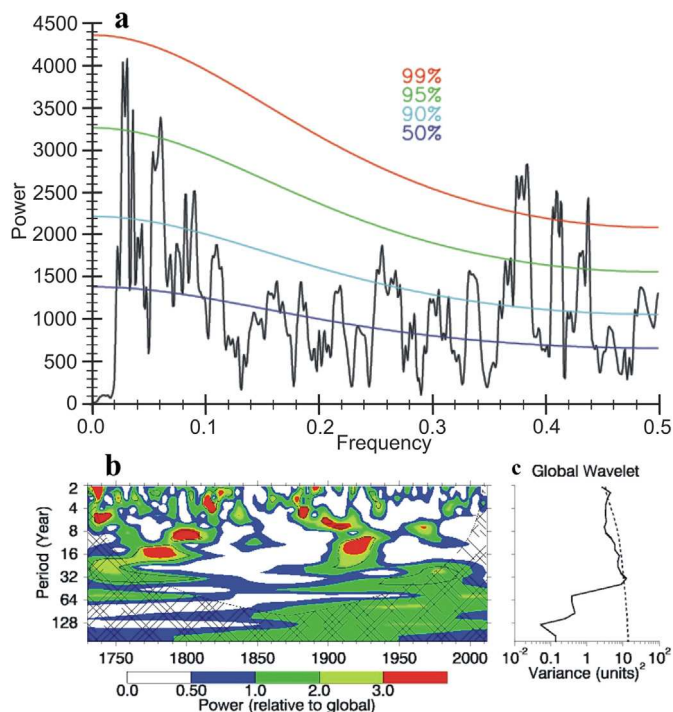


**Fig. 10.** (a) Multitaper power spectra of the reconstructed FM precipitation (AD 1730–2012). (b) Morlet wavelet spectrum for reconstructed FM precipitation (AD 1730–2012). Black contours in the power spectrum represent the 95% significance level based on red noise background. The cone shaped net depicts areas of the spectrum where edge effects become important (Torrence and Compo, 1998). (c) Global wavelet power spectrum. (For interpretation of the references to colour in this figure legend, the reader is referred to the web version of this article.)

extended droughts of the pre-instrumental era recorded in the 1740s, 1780s, and 1840s were noted to be widespread in the western Himalaya. Pluvial phases were recorded in the 1730s, 1750s, 1806–1810, 1823–1834, 1860s, 1880s, 1910s, and 1980s. Such reconstructions using larger tree-ring data network should help in understanding regional-scale precipitation patterns, required for improving predictive skill.

## Acknowledgements

RRY and KGM thank the Director, Birbal Sahni Institute of Palaeobotany, Lucknow for facilities. BSK thanks ISRO-GBP for funding. The authors express sincere thanks to two anonymous reviewers for critical suggestions which greatly improved the paper.

## References

- Atkinson, E.T., 1882. *The Himalayan Gazetteer*. Cosmo Publications, New Delhi (Reprint 1973).
- Borgaonkar, H.P., Pant, G.B., Rupa Kumar, K., 1994. Dendroclimatic reconstruction of summer precipitation at Srinagar Kashmir, India since the late 18th century. *The Holocene* 4, 299–306.
- Bräuning, A., 2004. Tree-ring studies in the Dolpo-Himalaya (western Nepal). *TRACE-Tree-Rings in Archaeology, Climatology and Ecology* 2, 8–12.
- Champion, H.G., Seth, S.K., 1968. *A Revised Survey of Forest Type of India*. Manager of Publications, Delhi.

- Cook, E.R., 1985. *A Time Series Approach to Tree-ring Standardization* (Ph.D. thesis). University of Arizona, Tucson, Arizona, USA.
- Cook, E.R., Peters, K., 1981. The smoothing spline: a new approach to standardizing forest interior tree-ring series for dendroclimatic studies. *Tree-Ring Bulletin* 41, 45–53.
- Cook, E.R., Peters, K., 1997. Calculating unbiased tree-ring indices for the study of climatic and environmental change. *The Holocene* 7, 361–370.
- Cook, E.R., Krusic, P.J., Jones, P.D., 2003. Dendroclimatic signals in long tree-ring chronologies from the Himalayas of Nepal. *International Journal of Climatology* 23, 707–732.
- Cook, E.R., Meko, D.M., Stahle, D.W., Cleaveland, M.K., 1999. Drought reconstruction for the continental United States. *Journal of Climate* 12, 1145–1162.
- Cook, E.R., Palmer, J.G., Ahmed, M., Woodhouse, C.A., Fenwick, P., Zafar, M.U., Wahab, M., Khan, N., 2013. Five centuries of Upper Indus River flow from tree rings. *Journal of Hydrology* 486, 365–375.
- Dawadi, B., Liang, E., Tian, L., Devkota, L.P., Yao, T., 2013. Pre-monsoon precipitation signal in tree-rings of timberline *Betula utilis* in the central Himalayas. *Quaternary International* 283, 72–77.
- Dubey, B., Yadav, R.R., Singh, J., Chaturvedi, R., 2003. Upward shift of Himalayan pine in western Himalaya, India. *Current Science* 85, 1135–1136.
- Fritts, H.C., 1976. *Tree-rings and Climate*. Academic Press, London.
- Gray, S.T., Graumlich, L.J., Betancourt, J.L., Pederson, G.T., 2004. A tree-ring based reconstruction of the Atlantic Multidecadal Oscillation since 1567 A.D. *Geophysical Research Letters* 31, L12205. <http://dx.doi.org/10.1029/2004GL019932>.
- Holmes, R.L., 1983. Computer-assisted quality control in tree-ring dating and measurement. *Tree-Ring Bulletin* 43, 69–78.
- Knight, J.R., Allan, R.J., Folland, C.K., Vellinga, M., Mann, M.E., 2005. A signature of persistent natural thermohaline circulation cycles in observed climate. *Geophysical Research Letters* 32, L20708. <http://dx.doi.org/10.1029/2005GL024233>.
- Mann, M.E., Lees, J.M., 1996. Robust estimation of background noise and signal detection in climatic time series. *Climate Change* 33, 409–445.
- Oldenborgh, G.J., Burgers, G., 2005. Searching for decadal variations in ENSO precipitation teleconnections. *Geophysical Research Letters* 32, L15701. <http://dx.doi.org/10.1029/2005GL023110>.
- Raspopov, O.M., Dergachev, V.A., Kolstrom, T., 2004. Periodicity of climate conditions and solar variability derived from dendrochronological and other palaeoclimatic data in high latitudes. *Palaeogeography Palaeoclimatology Palaeoecology* 209, 127–139.
- Sati, V.P., 2005. Systems of agriculture farming in the Utranchal Himalaya, India. *Journal of Mountain Science* 2, 76–85.
- Singh, J., Yadav, R.R., 2005. Spring precipitation variations over the western Himalaya, India since AD 1731 as deduced from tree rings. *Journal of Geophysical Research* 110, D01110. <http://dx.doi.org/10.1029/2004JD004855>.
- Singh, J., Park, W.-K., Yadav, R.R., 2006. Tree-ring-based hydrological records for western Himalaya, India, since AD 1560. *Climate Dynamics* 26, 295–303.
- Singh, J., Yadav, R.R., Wilmking, M., 2009. A 694-year tree-ring based rainfall reconstruction from Himachal Pradesh, India. *Climate Dynamics* 33, 1149–1158.
- Singh, J., Yadav, R.R., Dubey, B., Chaturvedi, R., 2004. Millennium-long ring-width chronology of Himalayan cedar from Garhwal Himalaya and its potential in climate change studies. *Current Science* 86, 590–593.
- Stokes, M.A., Smiley, T.L., 1968. *An Introduction to Tree-ring Dating*. University of Chicago Press.
- Torrence, C., Compo, G.P., 1998. A practical guide to wavelet analysis. *Bulletin of the American Meteorological Society* 79, 61–78.
- Wang, S.-Y., Yoon, J.-H., Gillies, R.R., Cho, C., 2013. What caused the winter drought in Western Nepal during recent years? *Journal of Climate* (in press) <http://dx.doi.org/10.1175/JCLI-D-12-00800.1>.
- Wigley, T.M.L., Briffa, K.R., Jones, P.D., 1984. On the average value of correlated time series with applications in dendroclimatology and hydrometeorology. *International Journal of Climatology* 8, 33–54.
- Yadava, R.K., Rupa Kumar, K., Rajeevan, M., 2012. Characteristic features of winter precipitation and its variability over the northwest India. *Journal of Earth System Sciences* 121, 611–623.
- Yadav, R.R., 2011a. Long-term hydroclimatic variability in monsoon shadow zone of western Himalaya, India. *Climate Dynamics* 36, 1453–1462.
- Yadav, R.R., 2011b. Tree-ring evidence of 20th century precipitation surge in monsoon shadow zone of western Himalaya, India. *Journal of Geophysical Research* 116. <http://dx.doi.org/10.1029/2010JD014647>.
- Yadav, R.R., 2013. Tree ring-based seven-century drought records for the Western Himalaya, India. *Journal of Geophysical Research, Atmosphere* 118. <http://dx.doi.org/10.1002/jgrd.50265>.
- Yadav, R.R., Park, W.-K., 2000. Precipitation reconstruction using ring width chronology of Himalayan cedar from western Himalaya: preliminary results. *Proceedings of the Indian Academy of Sciences (Earth and Planetary Sciences)* 109, 339–345.
- Yadav, R.R., Bhutiyani, M.R., 2013. Tree-ring-based snowfall record for cold arid western Himalaya, India since A.D. 1460. *Journal of Geophysical Research, Atmosphere* 118. <http://dx.doi.org/10.1002/jgrd.50583>.